

Efficacy of Endoscopic Transantral versus Transorbital Surgical Approaches in the Repair of Orbital BlowOut Fractures-(Randomized Clinical Trial).

Submitted To The Faculty Of Dentistry, Cairo University
In Partial Fulfillment Of The Requirement Of the Doctor Degree
In Oral And Maxillofacial Department

By

Nahla Mahmoud Awad-Allah

B.D.S (Faculty of Dentistry- Cairo university; 2008)

M.D.S (Faculty of Dentistry-Cairo university; 2015)

2018

Supervisors

Dr. Ibrahim Ezzat Shindy

Professor of Oral and Maxillofacial Surgery,
Faculty of Dentistry,
Cairo University.

Dr. Reem Hamdy Hossameldin

Lecturer in Oral and Maxillofacial Surgery,
Faculty of Dentistry,
Cairo University.

Dr. Samer Noaman Abdel-Gabar

Associate Professor of Oral and Maxillofacial Surgery,
Faculty of oral and Dental Medicine,
Sana's University.

Judgment Committee

Dr. Basma Gamal Moussa

Professor of Oral and Maxillofacial Surgery,
Faculty of Dentistry,
Cairo University.

Dr. Mohammed Daiaa Zein-elAbdeen

Professor in Oral and Maxillofacial Surgery,
Dean of Faculty of Dentistry,
Ain Shams University.

Dr. Ibrahim Ezzat Shindy

Professor of Oral and Maxillofacial Surgery,
Faculty of Dentistry,
Cairo University.

Dedication

This work is especially dedicated

To

- *The pure soul of my dad; your supporting arm always on my shoulder. Rest in peace dear father.*
- *To the source of love, care and support in my life: to my family.*

ACKNOWLEDGEMENT

My deepest thanks and gratitude goes to Dr. Ibrahim Ezzat Shindy, Professor of Oral and Maxillofacial Surgery, Faculty of Dentistry, Cairo University. My dearest professor: you have been really supportive, generous and responsible. Without your guidance this work would never be accomplished.

My deepest sense of gratitude goes to Dr. Reem Hossameldin, Lecturer in Oral and Maxillofacial Surgery, Faculty of Dentistry, Cairo University, for her kind supervision, valuable advices and continuous encouragement throughout the study.

No Words can express what I owe to Dr. Samer Noaman. Assistant Professor of Oral and Maxillofacial Surgery, Faculty of Medicine, Sana' University, whom I consider an integral part of this research for all what he has done. I am really appreciated.

*My great thanks to all **staff members** of Oral and Maxillofacial Surgery, Faculty of Dentistry, and Oculo-plastic surgery, faculty of medicine, Cairo University for helping me and giving me their experience throughout my work, their efforts will always be remembered.*

LIST OF FIGURES

NO	Figure	Page
(1)	Diagrammatic illustration of the right bony orbit.	2
(2)	Sagittal section of the left orbit showing the orbital floor, medial wall and the left maxillary sinus.	5
(3)	Schematic illustration of (A) The hydraulic theory, and (B) The buckling theory.	10
(4)	Diagrammatic illustration of, (A) The hydraulic theory and (B) The buckling theory	11
(5)	A diagram illustrating the upward sloping of the floor posteriorly in intact orbits (left). Loss of the normal configuration leads to sinking of the globe with a backward and downward displacement (right)	15
(6)	Screenshot of randomization process by Researcher Randomizer.	31
(7)	Clinical intra-operative photo showing (Preoperative Forced Duction Test (positive)).	33
(8)	Clinical intra-operative photo showing (Upper gingivobuccal incision is made allowing exposure of the maxilla for osseous cuts at the fracture site).	34
(9)	Clinical intra-operative photo showing (Arrow show the infraorbital foramen after dissection).	34
(10)	Clinical intra-operative photo showing (2 holes in the anterior maxillary wall were performed with an eggshell bur taking care to preserve the medial and lateral buttresses as well as the infraorbital nerve).	35
(11)	Sinus scope 4 mm, 30 degrees short one 17 cm.	35
(12)	Intra-operative endoscopic photo showing (Sinus membrane removal with curved hemostat for better visualization of herniated orbital content).	36
(13)	Intra-operative endoscopic views of the left maxillary sinus of an orbital floor fracture, through the antral window. The orbital floor was fractured, and periorbital soft tissue was herniated into the maxillary sinus (arrow).	36

(14)	Intraoperative endoscopic view of the fractured bony margin. Identification of the inferior orbital nerve (arrow).	37
(15)	Intraoperative endoscopic view of the fractured bony margins after reduction (arrows).	37
(16)	Intraoperative endoscopic view showing Reinforced collagen membrane was inserted into the maxillary sinus to support the reduced orbital floor.	38
(17)	Intra-operative endoscopic views of the left maxillary sinus of the reconstructed orbital floor fracture with collagen membrane, through the antral window. (arrow)	38
(18)	Clinical intra-operative photo showing (Postoperative Forced Duction Test (negative)).	39
(19)	Clinical intra-operative photo showing (The lower eyelid was everted with fine hemostat and 3 traction sutures (from the palpebral conjunctiva to the skin), approximately 4 to 5mm below the lid margin to ensure that the tarsal plate was included in the suture).	39
(20)	Clinical intra-operative photo showing (Incision of the conjunctiva below the tarsal plate. Periosteal incision; to facilitate this maneuver, another traction suture was placed through the cut end of the conjunctiva. By using the cautery the periosteal incision was performed down to the orbital bone).	40
(21)	Clinical intra-operative photo showing (Once the infraorbital rim was exposed; the periorbital dissection was performed till reaching the fractured bony margins, then reduction of the herniated orbital contents from the maxillary sinus to the orbit. (Arrow))	40
(22)	Clinical intra-operative photo showing (Identification of the inferior orbital nerve after orbital content reduction).	41
(23)	Clinical intra-operative photo showing (Reconstruction of the fractured orbital floor using 0.3 ready-made titanium mesh and 4 self-drilling titanium mini-screws)..	41
(24)	Clinical intra-operative photo showing (Postoperative forced duction test to ensure no muscles' entrapments through the mesh).	42
(25)	Clinical intra-operative photo showing (Closure of the tranconjunctival incision and the lateral canthotomy).	42

(26)	Case.1 Clinical photo showing (A) Preoperative left limited elevation due to muscle entrapment in orbital floor fracture site (left photo). (B) Postoperative photo after left orbital floor reconstruction.	47
(27)	Computed tomography (CT) scans of the blowout fracture of the inferior orbital wall. (A) Preoperative view. (B) Postoperative 2nd day CT. (C) Well reduced state of fractured bony wall 6 months post surgery.	47
(28)	Preoperative and postoperative ophthalmological examination.	48
(29)	Case.3 Clinical photo showing (A) Preoperative right limited elevation due to muscle entrapment in orbital floor fracture site. (B) Postoperative photo after right orbital floor reconstruction.	48
(30)	Computed tomography (CT) scans of the blowout fracture of the inferior orbital wall. (A) Preoperative view. (B) Postoperative CT.	48
(31)	Case.5 Clinical photo showing (A) Preoperative left limited elevation due to muscle entrapment in orbital floor fracture site. (B) Postoperative photo after left orbital floor reconstruction.	49
(32)	Case.1 Clinical photo showing (A) Preoperative left enophthalmos and limited elevation (B) postoperative photo showing resolution of enophthalmos and restriction of elevation.	49
(33)	Computed tomography (CT) scans of the blowout fracture of the inferior orbital wall. (A) Preoperative view. (B) Well reduced state of fractured bony wall 6 months post surgery.	49
(34)	Preoperative and postoperative ophthalmological examination.	50

(35)	Case.3 Clinical photo showing (A) Limited elevation (B) limited depression due to muscle entrapment. (C&D) Postoperative photos after orbital floor reconstruction.	50
(36)	Case.4 Clinical photo showing (A) preoperative marked left enophthalmos,(B) postoperative improvement with residual enophthalmos.	50
(37)	CONSORT flow diagram of the study	51
(38)	Bar chart representing post-operative diplopia resolution in the two groups (study group; control group).	53
(39)	Bar chart representing frequencies (n) and results of McNemar test for Enophthalmous Incidence in both groups.	53
(40)	Pie chart representing EMO limitations in the both groups.	54
(41)	Clinical photo showing (Periorbital edema (A) control case: 2nd day after surgery (B) endoscopic case: 2nd day after surgery	54

LIST OF TABLES

NO	Table	Page
(1)	Demographic data description regarding age and time lapse to surgery	52
(2)	Frequencies (n), percentages and results of fisher exact test for Diplopia Improvement for the tested groups.	52
(3)	Frequencies (n), and results of Mcnemartest for Enophthalmous:	53

LIST OF ABBREVIATIONS

Abbreviation	Meaning
EOM	Extra-ocular muscles
BOF	Blowout fracture
CT	Computerized tomography
SLIM	Superior, lateral, inferior, medial
(HDPE)	High density porous polyethylene
(PDS)	poly-d-dioxanone
GBR	Guided bone regeneration
PT	Prothrombin time
PTT	Partial thromoplastin time
INR	International normalized ratio
RAE	Right angle endotracheal tube
IM	Intramuscular
SPSS	Statistical Package for Social Sciences
SD	Standard deviation

CONTENTS

Title	Page
Introduction	1
Review Of Literature	2
Aim Of The Study	27
Patients And Methods	28
Results	51
Discussion	56
Summary	60
Conclusions And Recommendations	61
References	62
Appendices	----
Arabic Summary	----

INTRODUCTION

Orbital floor fracture is one of the most common facial skeleton fractures after mid facial trauma, accounting for up to 40% of cranio-facial injuries. Patients may complain of ocular symptoms, aberration of aesthetic appearance, and dysesthesia around the damaged cheek.¹

The indication for repair of orbital wall fractures is based on the clinical symptoms, exophthalmometry and computed tomography (CT). The timing of treatment, surgical technique and type of reconstruction material used is debated. Some advocate following the post trauma course for the development of diplopia or enophthalmos before starting treatment.²

Although a variety of approaches to orbital floor fractures have been proposed, satisfactory postoperative results have not been obtained in all cases. The key to successful surgical repair of these injuries is adequate exposure, visualization of the posterior bone shelf, and anatomical reconstruction of the entire defect. The traditional approach exposes the orbital floor, but it is difficult to see the posterior edge of the fracture and the condition of the herniated tissue before and after reduction of the orbital contents. Posterior dissection is the most difficult maneuver and is a common reason for failure of orbital floor repair.³

Transmaxillary endoscopic visualization of the orbital floor offers an excellent view of the entire defect and the surgical reconstruction.⁴

Several alternate materials used to support the orbital floor in the maxillary sinus via a transantral approach, include hydroxyapatite block, collagen membranes, silicone block, and balloon and gauze soaked with iodine formaldehyde. Potential problems with these methods are instability, implant displacement, inadequate reduction, infection, as well as cost.

REVIEW OF LITERATURE

Thorough knowledge of anatomy with topographical variants is of paramount importance to the surgeon in his everyday management of post-traumatic lesions of the orbit and peri-ocular area for optimal results. ⁶

A-The bony orbit:

The orbits are paired structures, located on the anterior part of the face. Morphologically, each orbit is a four sided pyramid with a posterior apex and anterior base. ⁷ the average dimensions of each orbit are 40 mm wide, 35 mm high and 40-50 mm deep. The angle between both lateral walls of both orbits is 90° and between the lateral and medial walls of the same side is 45. The medial walls are almost parallel to the sagittal plane. ⁸ There are seven bones forming each orbit: frontal, ethmoid, lacrimal, sphenoid, zygomatic, palatine, and maxilla (**fig. 1**). ⁷

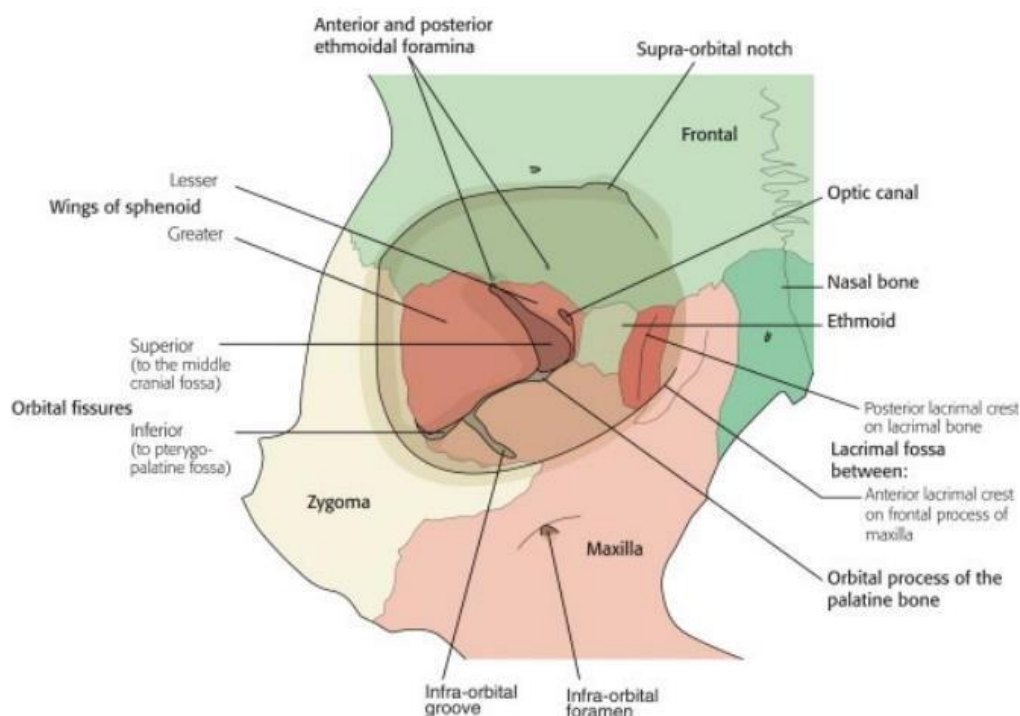


Fig. (1): Diagrammatic illustration of the right bony orbit. ⁹

The orbital roof is the floor of the anterior cranial fossa and the frontal sinus and is formed by the orbital plate of the frontal bone. The orbital surface of the zygomatic bone and greater wing of the sphenoid constitute the lateral wall. The medial wall is made (from anterior to posterior) from the frontal process of the maxillary bone, the lacrimal bone and the lamina papyracea of the ethmoid bone with a small contribution by the lesser wing of the sphenoid. The floor is formed by the orbital surfaces of the zygomatic bone and maxilla, and minimally by the Palatine bone. The zygomatic, frontal and maxillary bones form the orbital margin. Medially the superior orbital rim ends of the spine of the lacrimal bone lying posterior to the inferior orbital margin, which ends of the spine of the maxillary bone. The fossa of the lacrimal sac is between these two spines.¹⁰

In general, the bone is thickest at the apex, thins as the walls diverge anteriorly, and then thickens again at the rims on the surface of the face. Although the bone of the medial orbital wall is thinnest, followed by the bone on the floor of the orbit, the medial wall is strengthened by the perpendicular septa of the ethmoid sinuses. The floor of the orbit is most vulnerable to fracture when there is a direct force exerted on the eye globe because it is thin and unsupported.^{11,12}

None of the walls of the orbit are flat; they are curvilinear in shape, and their purpose is to maintain the projection of the globe and to cushion it when subjected to blunt force.¹² The orbital floor is almost triangular with rounded corners being narrower posterior. The floor is not horizontal but slopes upwards and medially at 45° and ascends posterior at about 30°, to terminate as the anterior margin of the inferior orbital fissure. At this point the bone curves abruptly downwards into the infra-temporal fossa to form the posterior wall of the maxillary antrum.¹³ Recreating this gentle curvature when repairing orbital floor fractures is important to restore normal anatomy and to prevent postoperative enophthalmos or proptosis.^{11, 13}